Fine tuning Exo2, a small molecule inhibitor of secretion and retrograde trafficking pathways in mammalian cells.

Lucie J. Guetzoyan[a], Robert A. Spooner[b], Frédéric Boal[c], David J. Stephens[c], J. Michael Lord[b], Lynne M. Roberts[b], Guy J. Clarkson[a].

Received (in XXX, XXX) Xth XXXXXXXXX 200X, Accepted Xth XXXXXXXXX 200X
First published on the web Xth XXXXXXXXX 200X
DOI: 10.1039/b000000x

The small molecule 4-hydroxy-3-methoxybenzaldehyde (5,6,7,8-tetrahydro[1]benzothieno[2,3-d]pyrimidin-4-yl)hydrazone (Exo2) stimulates morphological changes at the mammalian Golgi and *trans*-Golgi network that are virtually indistinguishable from those induced by brefeldin A. Both brefeldin A and Exo2 protect cells from intoxication by Shiga(-like) toxins by acting on other targets that operate at the early endosome, but do so at the cost of high toxicity to target cells. The advantage of Exo2 is that it is much more amenable to chemical modification and here we report a range of Exo2 analogues produced by modifying the tetrahydrobenzothienopyrimidine core, the vanillin moiety and the hydrazone bond that links these two. These compounds were examined for the morphological changes they stimulated at the Golgi stack, the *trans* Golgi network and the transferrin receptor-positive early endosomes and this activity correlated with their inherent toxicity towards the protein manufacturing ability of the cell and their protective effect against toxin challenge. We have developed derivatives that can separate organelle morphology, target specificity, innate toxicity and toxin protection. Our results provide unique compounds with low toxicity and enhanced specificity to unpick the complexity of membrane trafficking networks.

.

Introduction

Membrane and vesicular transport is fundamental to the organization and function of all eukaryotic cells. Newly synthesised proteins for secretion are transported between the intracellular compartments of the endoplasmic reticulum (ER), Golgi apparatus and *trans*-Golgi network (TGN) using a defined set of vesicular and tubular intermediates whose formation is tightly controlled by a series of regulatory proteins. A reverse pathway likewise involves the regulated formation of transport intermediates that traffic internalized proteins from the plasma membrane via the complex endosomal system and on to either lysosomes or, in the 'retrograde' pathway, the TGN, Golgi and ER.[1, 2] A cartoon depicting an overview of the course of membrane transport is shown in Figure 1. Some protein toxins highjack the retrograde route to reach the ER and deliver their lethal cargo (*e.g.* the bacterial cholera and Shiga-(like) toxins and plant toxin ricin) yet have been invaluable in the description of the steps and key regulatory proteins that operate in these pathways.[3-8] Chemical intervention with small molecule inhibitors of trafficking has also played a role but these are often pleiotropic in their action and their effects are accompanied by high levels of (often unreported) toxicity (*vide infra*). Molecules with more specific activity and low inherent toxicity towards treated cells could finesse greater detail, understanding and control of trafficking processes.

To date, the fungal metabolite brefeldin A (BFA, Fig. 1) is the best characterized inhibitor of both secretion and toxin retrograde transport.[9, 10] It promotes the complete disruption of the Golgi apparatus and the fusion of Golgi and ER compartments. It also significantly disrupts the structure of the TGN, promoting the tubulation and merging of the TGN and endosomal compartments. The structure of BFA and a cartoon depiction of these effects are shown in the left hand lane of Figure 1. BFA targets at least three guanine nucleotide exchange factors (GEFs) that regulate the activity of members of the ADP Ribosylation Factor (Arf) family of small GTPases.[11] These are required for the concentration of cargo and the formation of coated transport carriers from various intracellular compartments such as the TGN, Golgi and early endosomes (EE). Arf1 is a critical trigger of coated carriers in the secretory and retrograde transport pathways where there are three known Arf1-specific GEFs: the Golgi-specific GBF1 and the TGN/endosomal BIG1 and BIG2 proteins.[12, 13] BFA inhibits all three by binding at the interface between a GDP bound Arf (GDP-Arf) and its GEF, stabilising an abortive GDP-Arf/Arf-GEF complex.[14] It also inhibits activation of Arf3[15] and Arf4[16] via their family of

[a]*Department of Chemistry, and* [b] *Department of Biological Sciences, University of Warwick, Coventry CV4 7AL, UK;*
[c] *Cell Biology Laboratories, Department of Biochemistry, University of Bristol, School of Medical Sciences, University Walk, Bristol BS8 1TD, UK*
E-mail: guy.clarkson@warwick.ac.uk
† Electronic Supplementary Information (ESI) available: Experimental data, protein synthesis data, protein synthesis data in chart format, microscopy pictures.

Arf-GEFs, highlighting the pleiotropic nature of this inhibitor. The mechanism of interfacial inhibition, where protein-protein interactions are stabilized to give a non-productive complex,[17] as opposed to drug-induced inhibition of productive complexes, has been proposed as an attractive way to treat human disease.[18, 19]

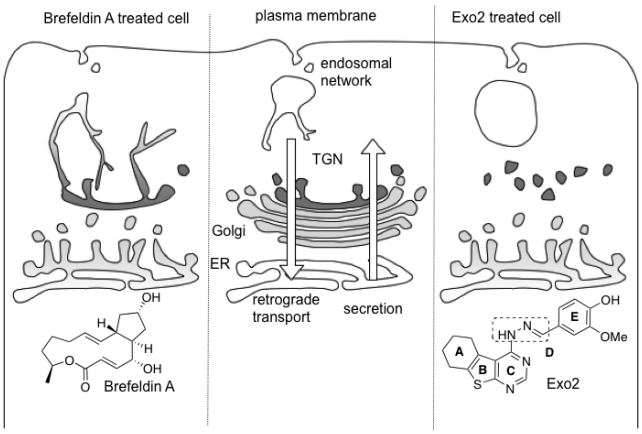

Figure1. Cartoon depicting the course of membrane transport in cells and the morphological effects of Brefeldin A and Exo2.

Several small molecule inhibitors of membrane transport have now been discovered from chemical genetics screens[7, 20-27] or by *in silico* approaches.[18] One of these molecules, 4-hydroxy-3-methoxybenzaldehyde (5,6,7,8-tetrahydro[1]-benzothieno-[2,3-d]pyrimidin-4-yl)hydrazone[28] (Exo2) is BFA-like in many respects, halting protein secretion and prompting similar morphological changes. Likewise, Exo2 induces complete disruption of the Golgi apparatus, fusion of Golgi and ER compartments[29] and significantly disrupts the structure of the TGN, but it does not promote the tubulation and merging of the TGN and endosomal compartments typical of treatment with BFA.[30] Thus it appears to interact with a subset of the GDP-Arf/Arf-GEF targets of BFA.[30] The structure of Exo2 and a cartoon depiction of the morphological changes brought about by Exo2 treatment of cells is shown in the right hand lane of Figure 1.

Both BFA and Exo2 exhibit a strong protective effect against intoxication by the Shiga toxins,[30, 31] major virulence factors produced by the dysentery-causing bacterium *Shigella dysenteriae*[32] and by enterohemorrhagic strains of *E. coli*, including the infamous food-poisoning serotype O157:H7.[33] These toxins normally traffic from the cell surface, via EE, the TGN and the Golgi, to the ER, where the homopentameric receptor-binding B chain complex and the cytotoxic A chain are separated. The A chain then retrotranslocates the ER membrane to enter the cytosol where it inhibits protein synthesis by depurinating a specific adenosine of the 28S RNA in the large ribosomal subunit.[8] Exo2 blocks the retrograde trafficking of these toxins at the EE–TGN interface.[30]

Due to its modular synthesis,[30] we were able to produce a range[34] of Exo2 analogues in an attempt to enhance these attributes. The compounds were individually screened for their effect on organelle morphology and function, target specificity, innate toxicity and their ability to protect cells against an acute challenge of *E. coli* Shiga-like toxin I (SLTx). We have identified the functional groups that are critical for the activity of Exo2 and tailored this activity to design new molecules with both enhanced target specificity and reduced inherent toxicity.

Results

Chemistry

Brefeldin A and Exo2 are shown in Figure 1. To help illustrate our approach to a structure activity-relationship (SAR) study based on Exo2, we have described Exo2 in terms of rings A, B, C and E and the hydrazone linker group D (Figure 1). Initial studies focused on altering the fused tricyclic pyrimidine core ABC involving modifications to the A ring and substitution on the pyrimidine ring C. The hydrazone link D was replaced by amine and triazole functionalities. Finally, the importance and nature of the substituents on ring E of the hydrazone was determined.

The intermediates made on route to generating the modifications to the tricyclic thienopyrimidone ring system are shown in Scheme 1. The thienopyrimidones **5-8,16** were obtained using a similar synthetic route as described for Exo2.[30] Using the Gewald reaction,[35] commercial ketones were condensed with ethyl cyanoacetate in the presence of sulphur to give the aminothienyl esters **1**-**4**. Cyclisation of the esters in formamide produced the thienopyrimidones **5**-**8**. The hydrazine derivatives **9**-**12** were obtained in two steps from the pyrimidones **5**-**8** using previously published conditions.[30] The final step was the condensation of the hydrazines **9**-**12** with vanillin to afford Exo2 and compounds **13**-**15** comprising of larger alkyl rings and ring cleaved analogues of Exo2. In a similar manner, cyclisation of **1** in acidic acetonitrile gave the methyl pyrimidone **16**, conversion to hydrazine **17** and reaction with vanillin gave **18**, a C ring substituted Exo2 analogue.

Attention then turned to the hydrazone linker group D. Initially, we examined the simple amino analogue **20** of Exo2 synthesised by the reaction of chloride **19** with tyramine (Scheme 2). Unfortunately, cells treated with **20** showed a large reduction in protein synthesis ability (see later) and this toxicity lead us to discount any further research in this line of analogues. We have previously published results detailing the oxidation and rearrangement of the hydrazone linker of Exo2 derivatives leading to fused 1,2,4-triazolopyrimidines.[36] Although these derivatives showed less inherent toxicity, they exhibited no morphological effects, had low solubility and little protective ability against STLx challenge. Concerned that the fused pyrimidine triazole ring system presented the E ring of these Exo2 analogues in an inappropriate orientation (see Figure 2), we now synthesised non-fused triazole analogues accessible *via* "click chemistry".[37] Our approach to these derivatives is shown in Scheme 3. Alkyne **21** was available via Sonogashira coupling between the chloride **19** and ethynyltrimethylsilane. Deprotection using TBAF gave the alkyne component **22**. The azide partner for the formation of a "click"analogue of Exo2 was obtained in two steps from 4-nitroguaiacol **23** which was reduced to the corresponding

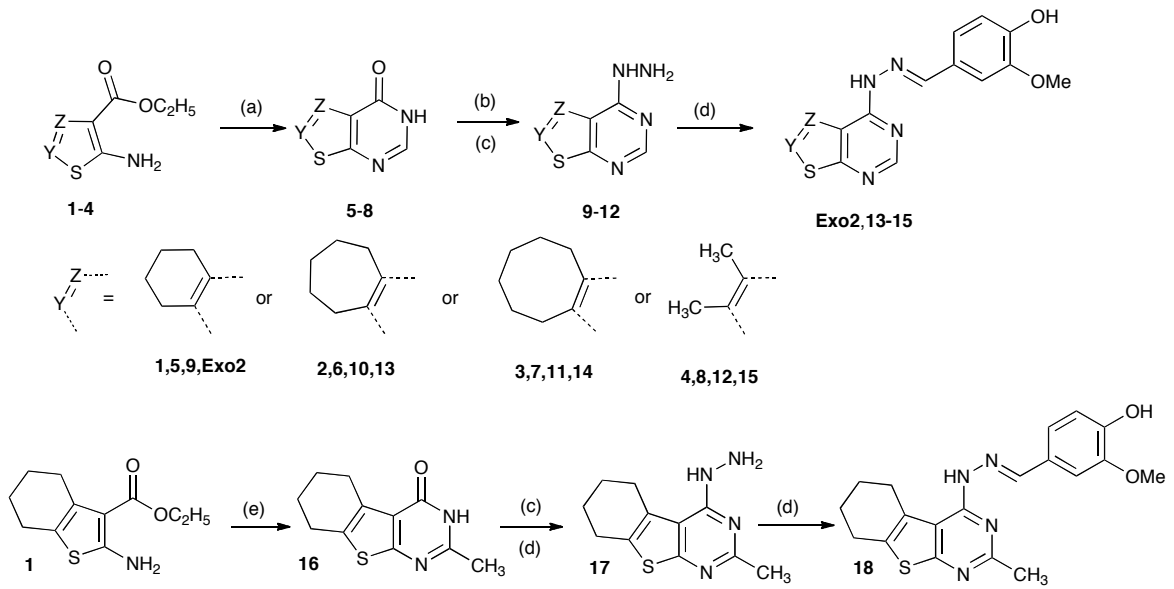

Scheme 1. Synthesis of A and C ring analogues of Exo2 (a) formamide, heat; (b) $POCl_3$, DMF, rt, 18hr, 30-80%; (c) hydrazine monohydrate, MeOH, rt, 2hr, 60-80%; (d) vanillin, MeOH, 40-90%; (e) cat. conc. HCl, acetonitrile, 85°C, 54%.

amine **24**[38] and then converted to the azide **25**.[39] Benzylic azides **26-28** were synthesized from the appropriate hydroxybenzyl alcohol,[40] and the same methodology was applied to afford the benzylic azide **29** after reduction of vanillin with $NaBH_4$. Finally the copper(I) catalyzed version of the azide-acetylene Huisgen 1,3-dipolar cycloaddition[37] was carried out to afford the 1,2,3-triazole analogues **30-34**. The regiochemistry of the cyclisations were confirmed by correlation spectroscopy which showed the expected NOE interactions between the triazole CH and the *ortho* protons of ring E.

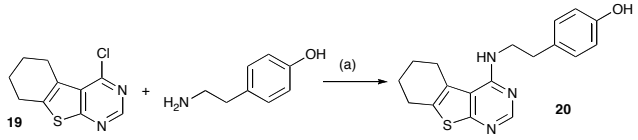

Scheme 2. (a) Et_3N, iPrOH, 90°C, 18hr, 60%

Attention then turned to alterations on ring E where rapid access to a family of compounds to gauge the importance of the position and nature of the substituents on ring E was available from a library of hydrazone derivatives. Hydrazones **35a-r** and **35w-z** were prepared from condensation of **9** with commercially available aldehydes (Table 3) and the others synthesized via a short route starting from 4-allyloxy-3-hydroxybenzaldehyde **36**.[41] Using allyl as a protecting group[42] following a sequence of alkylation to give the ethers **37a-c** and then deprotection gave the 3-alkyloxy-4-hydroxy substituted aldehydes **38a-c** (Scheme 4). Aldehydes **38a-c** were finally condensed with **9** to afford the hydrazone analogues **35s-v**. The compounds shown in Table 3 probe the importance of the substituent(s) and their orientation on ring E and comprise of an Exo2 isomer (**35a**), various hydroxy and methoxy analogues (**35b** to **35*l***), a random selection of substituents (**35m** to **35r**), an investigation of the *meta* alkoxy chain length (**35s** to **35v**) and finally possible hydroxy isosteres (**35w** to **35z**).

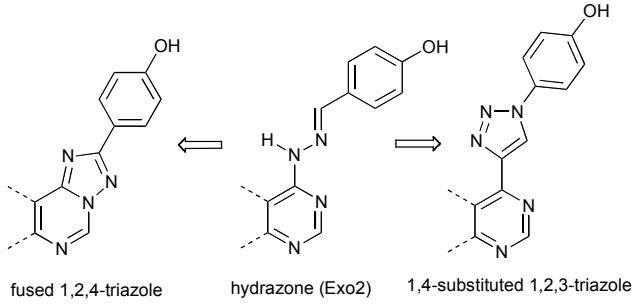

Figure 2. Possible triazole mimics of the hydrazone link

Biological testing.

Exo2 treatment of HeLa cells causes the fusion and swelling of the endosomes and blocks egress of SLTx from EE to the TGN.[30] We therefore probed the viability of this retrograde trafficking pathway in cells treated with Exo2 and these derivatives by examining their individual abilities to protect these cells from intoxication by SLTx. HeLa cells were treated with a fixed dose (50 $ng.ml^{-1}$) of SLTx in medium containing either vehicle DMSO or 50μM compound diluted from DMSO, conditions already established for Exo2,[30] after which protein synthesis ability was determined by measuring incorporation of [^{35}S]-methionine into acid-precipitable material (PST, Tables 1, 2 and 3). Results for each compound were normalized to coeval controls that measured the protein synthesis ability of cells treated with compound alone (PS, Tables 1, 2, 3 and Charts 1S, 2S, 3S in SI). These figures are shown in the related tables and as a comparison, compound efficacy (χ) is quantified as a protective effect calculated as the ratio of protein synthesis remaining after treatment with compound and SLTx toxin challenge compared to protein synthesis on treatment with compound alone. The latter reveals the impact of the compound itself on the protein synthesis capability of the cells. For example, although only ~42% protein synthesis ability remains in cells treated with

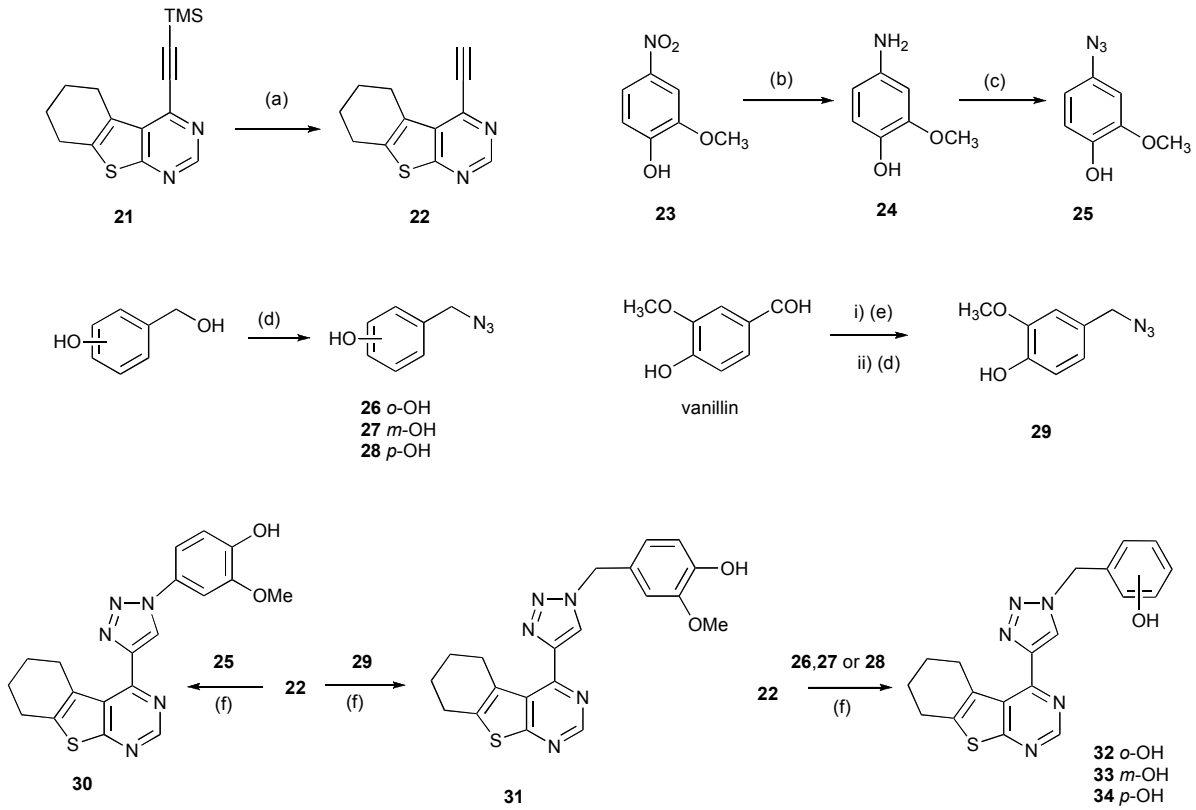

Scheme 3. Synthesis of 1,4-triazine analogues of Exo2 (a) TBAF, THF, 90%; (b) H_2, 10% Pd/C, EtOH, 90%; (c) $NaNO_2$, NaN_3, HCl(aq), (d) PPh_3, NaN_3, DMF / CCl_4 (4:1), 43-60%; (e) $NaBH_4$, THF, 66%; (f) $CuSO_4.5H_2O$, sodium ascorbate, EtOH / H_2O / THF (1:1:1), 30-60%.

Exo2 alone (PS, Table 1, Chart 1S in SI), ~41% remains in cells treated with Exo2 and SLTx (PST, Table 1), so the latter cells retain ~95% of their protein synthesis ability following toxin treatment (χ, Table 1). Thus Exo2 has high efficacy against SLTx challenge. In contrast, the vehicle DMSO, whilst having no effect on protein synthesis ability by itself, has a small protective effect against SLTx, with ~39% protein synthesis ability remaining after toxin challenge. The small protective effect of DMSO has been noted before,[43] and has been attributed to decreased fluidity of membranes which reduces toxin delivery.

The morphological changes stimulated by Exo2 are believed to be responsible for its protective effect against a SLTx challenge but also its inherent toxicity.[30] Thus, protection against incoming toxin might correlate with

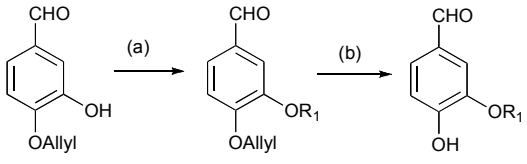

Scheme 4. Synthesis of *meta* alkoxy, *para* hydroxy aldehydes (a) K_2CO_3, DMF, R_1-Br, rt, 18hr, 51-70%; (b) $Pd(OAc)_2$, PPh_3, HCOOH, 90°C, 6hr, 25-75%

toxicity of the compound. It is immediately apparent from the numbers in the tables and shown pictorially in Charts 1S, 2S and 3S in SI that there is no clear link between the ability to protect against SLTx and the innate toxicity of each compound, suggesting that more selective inhibitors exist amongst these derivatives.

In parallel, we examined the morphological changes stimulated by these compounds. Fixed cells were stained for the TGN marker TGN46[44] and the Golgi marker giantin[45] (Figure 1S in SI), and examined by widefield microscopy. Cells treated with DMSO have a ribbon–like TGN and perinuclear Golgi, whilst in cells treated with Exo2 both of these structures are widely dispersed, leaving just a few remaining punctae.[30] An intermediate state between these morphologies is exemplified by compound **35l** (see Table 3 and Figure 1S in SI) which has a partial disruption of both TGN and Golgi structures, with replacement of ribbon-like perinuclear structures with numerous punctuate structures. Designating a DMSO-like phenotype as 'D', an Exo2-like phenotype as 'E' and an intermediate effect as 'I', we characterised the Exo2 analogues as detailed in the relevant Tables. We also examined the appearance of transferrin receptor (TnfR)-positive early endosomes after challenge with DMSO, Exo2 and Exo2 analogues, noting in a similar manner 'D' (DMSO-like, normal endosomal appearance), 'E' (Exo2-like, swollen endosomes) and an intermediate effect as 'I' (Table 1, 2 and 3 and Figure 1S in SI). The endosomal 'E' phenotype differs from that stimulated by BFA treatment which causes endosomal tubulation (Figure 1S in SI). None of the compounds tested generated a BFA phenotype at the transferrin receptor (TnfR)-positive early endosomes.

Table 1. **Table 1.** Modification of the alkylthienopyrimidine rings ABC

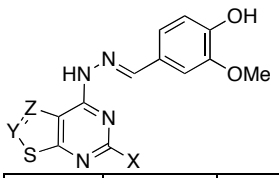

	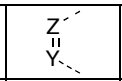	X	Golgi	TnfR	PS	PST	(χ)
DMSO	-	-	D	D	100	39.3	39.3
Exo2	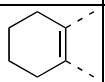	H	E	E	42.1	40.7	96.8
13	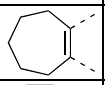	H	E	E	16.6	16.2	97.6
14	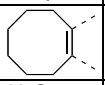	H	E	D	9.4	9.2	97.6
15	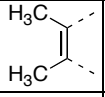	H	D/I	D	65.6	42.1	64.1
18	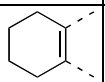	CH_3	I	D	41.6	24.4	58.6

TGN and Golgi phenotypes: D, DMSO-like; I, intermediate; E, Exo2-like. TnfR+ endosome phenotypes: D, DMSO-like; E, Exo2-like. PS: protein synthesis compound only, PST: protein synthesis with toxin challenge. (χ) protective coefficient (%)

Modification of the alkylthienopyrimidine core ABC

A range of compounds were prepared varying the alkylthienopyrimidine core of Exo2 and tested for their ability to inhibit SLTx transport compared with their inherent toxicity and characterised by their effects on the morphologies of the TGN/Golgi and endosomes (Table 1 and Chart S1 in SI). Increasing the cycloalkane ring size to seven (**13**) and eight carbons (**14**) retains a similar protective effect (χ) ratio but shows a steep increase in toxicity with an accompanying erosion of an Exo2 phenotype. Clipping ring A, analogue **15** has less inherent toxicity but a reduced protective effect against SLTx and again showing reduced morphological effects. Substitution on the pyrimidine ring (**18**) was similarly disadvantageous. These changes on the alkythienopyrimidine core were detrimental and highlight the importance of this structural region of Exo2 for eliciting both a protective effect and phenotypic response. This suggests that the binding site cleft of the Exo2 target(s) is relatively restricted and cannot easily accommodate the larger cycloheptenyl or cyclooctenyl rings of compounds **13** and **14**, but also shows a weaker interaction with the shorter core of **15**.

Modifications of the hydrazone link D

Exchange of the hydrazone NH-N=CH fragment of Exo2 with aminoethyl NH-CH_2-CH_2 gave compound **20** that exhibited very high toxicity drastically reducing protein synthesis ability and exhibiting no morphological effects dissuading us from further study of this group as a hydrazone replacement. We have previously reported an alternative modification involving the synthesis of a series of fused 1,2,4-triazole Exo2 derivatives (see Figure 2) obtained by oxidative cyclisation of the precursor hydrazones.[36] These molecules unfortunately did not protect against SLTx challenge. As the ring fused triazole skeletons may not present the E ring and its substituents in an optimal orientation for substrate binding, we synthesised 1,4-substituted triazoles (**30**-**34**) via the Huisgen 1,3-dipolar cycloaddition.[37] Although postulated as an amide isostere,[46] we considered the 1,4-substituted 1,2,3-triazole could also retain the appropriate geometry and suitable atoms to chemically mimic the hydrazone bond (see Figure 2). These triazole compounds consisted of both the analogous Exo2 derivative (**30**) and the benzyl analogues (**31**-**34**) (Scheme 4) that may allow extra degrees of freedom in presenting the key hydroxyl substituents (*vida infra*). Although all such modifications to Exo2 gave rise to molecules with low toxicity (Table 2, Chart 2S in SI), in all cases, exchange of the hydrazone bond for a 1,4-substituted triazole (**30**-**34**) was deleterious, with marked loss of ability to stimulate visible morphological changes at the TGN/Golgi

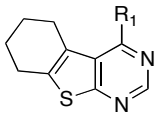

Table 2. Modification of the hydrazone group D

	R_1	Golgi	TnfR	PS	PST	(χ)
DMSO	-	D	D	100	39.3	39.3
Exo2	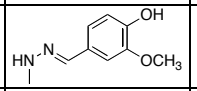	E	E	42.1	40.7	96.8
20	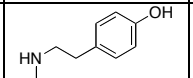	D	D	9.2	4.8	51.5
30	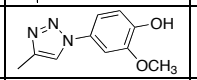	I	D	73.1	17.8	24.3
31	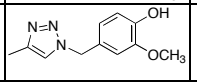	n.d.	n.d.	63.1	24.2	38.4
32	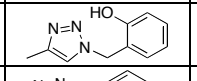	D	D	75.1	47.4	61.5
33	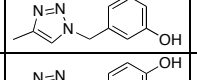	D	D	87.7	53.9	61.5
34	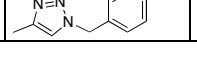	D	D	80.4	35.1	43.7

TGN and Golgi phenotypes: D, DMSO-like; I, intermediate; E, Exo2-like. TnfR+ endosome phenotypes: D, DMSO-like; E, Exo2-like; n.d., not determined. PS: protein synthesis compound only, PST: protein synthesis with toxin challenge. (χ) protective coefficient (%)

Table 3. Hydrazone formation and substituents on ring E ring

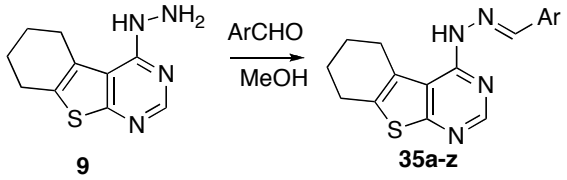

No	Ar	TGN Golgi	TnfR	PS	PST	(χ)	No	Ar	TGN Golgi	TnfR	PS	PST	(χ)
DMSO		D	D	100	39.3	39.3	**35m**		I	E	58.5	36.7	62.6
Exo2	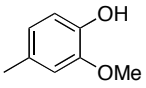	E	E	42.1	40.7	96.8	**35n**	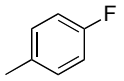	I	D	60.9	38.4	63.0
35a	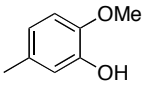	I	I	41.2	33.6	81.6	**35o**	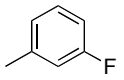	I	D	57.7	36.6	63.4
35b	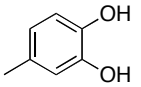	E	E	49.5	42.7	86.1	**35p**		I	D	77.0	34.1	44.3
35c	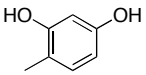	I/E	E	50.1	28.8	57.5	**35q**	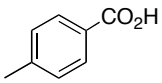			insoluble		
35d	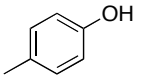	E	E	63.1	57.0	90.4	**35r**	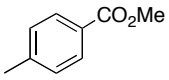	D	D	67.4	25.9	38.5
35e	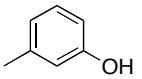	I	E	46.5	24.9	53.7	**35s**	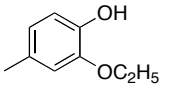	D	E	51.3	50.3	98.1
35f	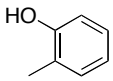	D	I	41.3	25.5	61.6	**35t**	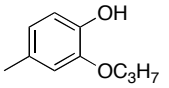	D	E	28.2	19.3	68.4
35g	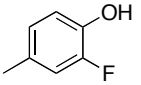	E	E	35.1	27.7	78.8	**35u**	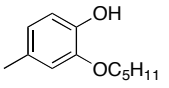	D	D	45.1	24.5	54.2
35h	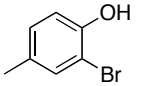	I/E	E	37.7	24.2	64.1	**35v**	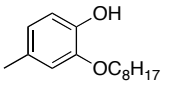	D	D	84.5	21.4	25.3
35i	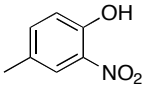	E	D	76.9	29.5	38.4	**35w**	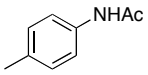	D	D	108.0	36.3	33.6
35j	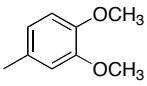	E	E	61.7	42.5	69.0	**35x**	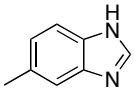	E	E	52.7	56.3	106.8
35k	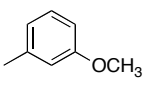	I/E	E	44.0	30.5	69.3	**35y**	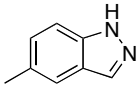	E	E	67.2	61.7	91.8
35l	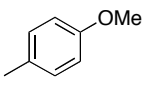	I	I	75.2	35.6	47.3	**35z**	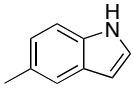	I	E	93.7	67.8	72.4

TGN/Golgi phenotypes: D, DMSO-like; I, intermediate; E, Exo2-like. TnfR+ endosome phenotypes: D, DMSO-like; E, Exo2-like. PS: protein synthesis compound only, PST: protein synthesis with toxin challenge. (χ) protective coefficient (%)

.

and the EE (Table 2). Only the *ortho* or *meta*-hydroxyl substituted benzyl triazoles **32** and **33** exhibited a modest efficacy against SLTx challenge. We postulate that the more flexible benzyl allows presentation of the *ortho* or *meta* hydroxyl groups in a more favourable orientation to compensate for the unfavourable positioning of the *para* hydroxy substituent of the more Exo2 like analogues **30**, **31** and **34** by the 1,4-triazole linker.

Modification of the substituents on ring E

As no dramatic effects were revealed by modification of the alkythienopyrimidine core and the hydrazone bond of Exo2, these moieties were used as a scaffold for a library of hydrazones examining the effect of the substituents on ring E and their orientation. The compounds, their phenotypic effects, protein synthesis and compound efficacy (χ) are shown in Table 3 (Chart 3S in SI) presented in a similar manner to the previous analogues. Generally a *para* hydroxyl substituent confers an Exo2-like phenotype at the EE and TGN/Golgi. Comparatively, *meta* and *ortho* hydroxy substituents show a reduced Exo2 phenotypic effect (e.g. the Exo2 isomer **35a** and the mono substituted **35e**, **35f**). A *meta* methoxy substituent can also elicit an Exo2 phenotypic effect (**35j**, **35k**) but with a reduced protective effect against SLTx challenge. Retention of the *para* OH and substitution of the *meta* methoxy substituent with longer alkyl ethers (**35s-35v**) initial gives an improvement with ethoxy analogue **35s** showing lower toxicity, an excellent efficacy (χ) and phenotypic effects focused at the EE. Further elongation of the ether chain quickly loses these benefits to give non-toxic inactive compounds (**35u**, **35v**). A similar loss of activity is also noted when exchanging the *meta* methoxy substituent for a fluorine (**35g**), bromine (**35h**) or to the larger nitro substituent (**35i**). Interestingly, though having no protective effect against SLTx, **35i** is able to generate an Exo2-like morphological effect at the TGN/Golgi as illustrated by the redistribution of the cis-Golgi marker GRASP 65,[47] and confirmed by the dissemination of another *cis*-Golgi marker NA-GFP,[48] without eliciting an effect at the EE. A similar but less specific phenotypic effect is demonstrated by fluoro analogues **35n** and **35o** and the pyridine derivative **35p**.

In view of the key *para* OH, we examined isostere replacement with an NH. This was originally disappointing as the acetamide **35w**, though of low toxicity exhibited no morphological changes or protective effect against SLTx. Concerned that the additional bulk of the acetyl group of **35w** was inhibiting receptor binding in a similar manner to the increase in size of the *meta* substituent detailed above, we developed the benzimidazole derivative **35x**. This still contains the NH but the steric bulk of the *meta* substituent is tied back in the 5-membered ring and the nitrogens of the benzimidazole **35x** are ideally situated to mimic the two oxygens of the phenol and methoxy of Exo2. Pleasingly, though benzimidazole derivative **35x** showed similar morphological effects to Exo2, it exhibited a lower toxicity profile and an excellent retention of protein synthesis after SLTx challenge. We promptly investigated the related indazole and indole analogues **35y** and **35z**. Compound **35y** had reduced toxicity and an excellent protective effect. Compound **35z** had protein synthesis levels approaching that of the control DMSO and retained more than 70% protein synthesis after SLTx challenge with morphological effects target predominantly at the endsosomes.

Figure 3 compiles all these toxicity and morphological data in a scatter plot of acute challenge with SLTx (protective effect) *versus* inherent compound toxicity, coding split circles for morphological changes stimulated at the TGN/Golgi (left-hand side of circles) and TnfR-positive EE (right-hand side of circles) as DMSO-like (white), intermediate (gray) or Exo-2 like (black). The majority of the compounds fall into three main groups: *Cluster 1*, predominately Exo2-like, *Cluster 2*, containing compounds with mixed features and *Cluster 3*, predominately DMSO-like. In addition, **35z** lies out with these clusters, having a good protective effect but being much less toxic than the other active Exo2 like compounds (*Cluster1*).

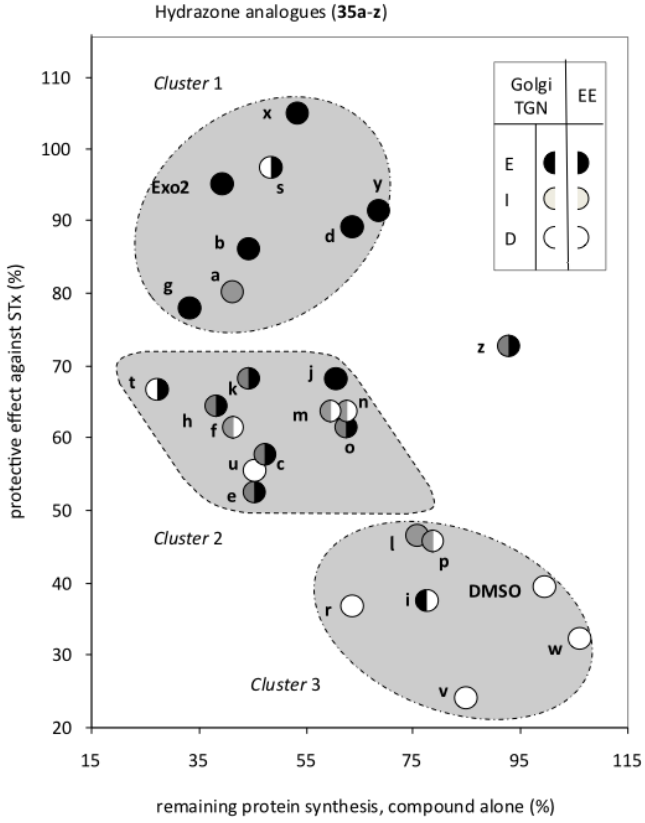

Figure 3. Scatter plot of protective effect against compound toxicity

Discussion

We have generated a range of Exo2 derivatives to determine structure-activity relationships, with key alterations that define Exo2 function and alter specificity. Here we report that Exo2 derivatives have differential effects on subcellular organelles, and propose that the alkylthienopyrimidine core, consisting of rings A, B and C anchors Exo2 in its target binding sites, and that the E ring is required for Exo2-like activity but also contributes towards innate toxicity. The differential effects on organelles imply either that Exo2 has multiple targets, or that there is one target that exhibits

varying affinities at the different sites.

At the level of light microscopy, none of the compounds tested differentiated between the Golgi and TGN, suggesting that these structures are linked intimately, with a common (set of) Exo2 target(s) which are responsible for maintaining both of these structures. We were unable to make any substantially dramatic changes to Exo2 at either the E ring, the A, B and C moiety or the hydrazone link D connecting them suggesting that both ends of the molecule and their relative orientation via the hydrazone are critical for engaging with Exo2 targets.

A *para*-hydroxyl group on ring E results in dissemination of TGN/Golgi structures and swollen endosomes, and strongly inhibits the retrograde trafficking pathway of SLTx (e.g. **35b**, **35d** and **35g)**. The protective effect of this *para*-hydroxyl group is context-dependent and can be eroded by increasing bulk of substituents at the *meta*-position highlighted by increasing the *meta* alkoxy chain length from ethoxy to octyloxy (**35s-v**). Mimicry of the *para*-hydroxyl group by a suitably positioned -NH of a heterocyclic ring (**35x-z**) produces Exo2 analogues with greatly reduced toxicity, more focused phenotypic effects and superior retention of protein synthesis after SLTx challenge, promising features for further investigation. There is no obvious structural relationship between Exo2 and BFA (Figure 1). However, the BFA cyclopentane ring carries a hydroxyl group that buries deeply within the Arf:Arf-GEF BFA-binding cleft, making specific contacts with both Arf and Arf-GEF.[49] The *para*-hydroxyl group of Exo2 that drives Exo2 activity may therefore make similar interactions with a subset of BFA sensitive targets, underlining the importance of the hydroxyl group and suggesting a possible orientation of Exo2 in such clefts. As well as modulating compound toxicity and protective effect, the nature of this substituent and its environment (*meta* substituent) also permit the tuning of these interactions with different targets. Clear candidates with differential specificity are **35s** and **35z**, which preferentially target the EE and **35i** which interferes at the Golgi/TGN.

The evidence that SLTx normally traffics through the Golgi stack is extensive. There are requirements for the small GTPase Arl1,[50] the Arl1 effector Golgi tethering factor golgin-97[50, 51] and the Arl1 targeting co-factor ARFRP1.[52] In addition, the Golgi tethering factors golgin-245[53] and GCC88,[54] the conserved oligomeric Golgi COG complex,[55] the Golgi-associated retrograde protein GARP[56] and the TGN tethering factor GCC185[57] control SLTx trafficking. Furthermore, roles for the Golgi docking and fusion promoter Rab6a[58, 59] and its RabGAP Rab6IP2[60] and for Rab11[57, 61] have been established. Physically, subcellular microsurgery to remove the Golgi stack halts retrograde transport of the SLTx B chain to the ER.[62] However, we demonstrate here that a visibly discrete Golgi structure is not an absolutely required for SLTx toxicity, since the dispersed Golgi fragments stimulated by **35i** are either competent for retrograde transport or the fused ER-Golgi induced by these compounds retains functionality for retrograde transport.

We conclude that there are at least two Exo2 targets, one operating at the TGN/Golgi and the other operational at the TnfR+ early endosomes. Organelle morphology and function can be separated by Exo2 derivatives. The alkylthienopyrimidine ring anchors Exo2 in the target binding sites, but the specificity of interaction with Exo2 targets and inherent toxicity can be altered by judicious substitution on the E ring of Exo2. Further work is now under way on the promising compounds reported here. The lower toxicity and specificity of these derivatives will allow a more rigorous characterization of cell transport and the opportunity to observe recovery pathways.

This work was generously supported by research grants from the Biotechnology and Biological Sciences Research Council (BB/E012450/1; to DS, GJC, LMR, JML) and the Wellcome Trust (080566Z/06/Z; to LMR, JML))

Notes and references

1. L. Johannes and V. Popoff, *Cell*, 2008, **135**, 1175-1187.
2. M. Pavelka, J. Neumuller and A. Ellinger, *Histochem. Cell Biol.*, 2008, **129**, 277-288.
3. L. Johannes and W. Romer, *Nat. Rev. Microbiol.*, 2010, **8**, 105-116.
4. P. O. Falnes and K. Sandvig, *Curr. Opin. Cell Biol.*, 2000, **12**, 407-413.
5. E. Fuchs, A. K. Haas, R. A. Spooner, S. Yoshimura, J. M. Lord and F. A. Barr, *J. Cell Biol.*, 2007, **177**, 1133-1143.
6. L. Johannes and B. Goud, *Traffic*, 2000, **1**, 119-123.
7. J. B. Saenz, T. A. Doggett and D. B. Haslam, *Infect. Immun.*, 2007, **75**, 4552-4561.
8. R. A. Spooner, D. C. Smith, A. J. Easton, L. M. Roberts and J. M. Lord, *Virol. J.*, 2006, **3**, 26.
9. R. D. Klausner, J. G. Donaldson and J. Lippincott-Schwartz, *J. Cell Biol.*, 1992, **116**, 1071-1080.
10. C. L. Jackson, *Subcell. Biochem.*, 2000, **34**, 233-272.
11. J. B. Helms and J. E. Rothman, *Nature*, 1992, **360**, 352-354.
12. H. W. Shin, N. Morinaga, M. Noda and K. Nakayama, *Mol. Biol. Cell*, 2004, **15**, 5283-5294.
13. X. Zhao, T. K. Lasell and P. Melancon, *Mol. Biol. Cell*, 2002, **13**, 119-133.
14. A. Peyroche, B. Antonny, S. Robineau, J. Acker, J. Cherfils and C. L. Jackson, *Mol. Cell*, 1999, **3**, 275-285.
15. S. C. Tsai, R. Adamik, R. S. Haun, J. Moss and M. Vaughan, *J. Biol. Chem.*, 1993, 268, 10820-10825.
16. L. A. Volpicelli-Daley, Y. Li, C. J. Zhang and R. A. Kahn, *Mol. Biol. Cell*, 2005, **16**, 4495-4508.
17. J. A. Wells and C. L. McClendon, *Nature*, 2007, **450**, 1001-1009.
18. J. Viaud, M. Zeghouf, H. Barelli, J. C. Zeeh, A. Padilla, B. Guibert, P. Chardin, C. A. Royer, J. Cherfils and A. Chavanieu, *Proc. Natl. Acad. Sci. U S A*, 2007, **104**, 10370-10375.
19. M. Zeghouf, B. Guibert, J. C. Zeeh and J. Cherfils, *Biochem. Soc. Trans.*, 2005, **33**, 1265-1268.
20. T. J. F. Nieland, Y. Feng, J. X. Brown, T. D. Chuang, P. D. Buckett, J. Wang, X. S. Xie, T. E. McGraw, T. Kirchhausen and M. Wessling-Resnick, *Traffic*, 2004, **5**, 478-492.
21. E. Macia, M. Ehrlich, R. Massol, E. Boucrot, C. Brunner and T. Kirchhausen, *Dev. Cell*, 2006, **10**, 839-850.
22. E. Fiebiger, C. Hirsch, J. M. Vyas, E. Gordon, H. L. Ploegh and D. Tortorella, *Mol. Biol. Cell*, 2004, **15**, 1635-1646.
23. J. B. Saenz, W. J. Sun, J. W. Chang, J. M. Li, B. Bursulaya, N. S. Gray and D. B. Haslam, *Nature Chem. Biol.*, 2009, **5**, 157-165.
24. H. E. Pelish, N. J. Westwood, Y. Feng, T. Kirchhausen and M. D. Shair, *J. Am. Chem. Soc.*, 2001, **123**, 6740-6741.
25. T. Hill, L. R. Odell, J. K. Edwards, M. E. Graham, A. B. McGeachie, J. Rusak, A. Quan, R. Abagyan, J. L. Scott, P. J. Robinson and A. McCluskey, *J. Med. Chem.*, 2005, **48**, 7781-7788.
26. Y. Feng, S. Yu, T. K. R. Lasell, A. P. Jadhav, E. Macia, P. Chardin, P. Melancon, M. Roth, T. Mitchison and T. Kirchhausen, *PNAS*, 2003, **100**, 6469-6474.

27. B. Stechmann, S. K. Bai, E. Gobbo, R. Lopez, G. Merer, S. Pinchard, L. Panigai, D. Tenza, G. Raposo, B. Beaumelle, D. Sauvaire, D. Gillet, L. Johannes and J. Barbier, *Cell*, 2010, **141**, 231-242.
28. J. C. Yarrow, Y. Feng, Z. E. Perlman, T. Kirchhausen and T. J. Mitchison, *Comb. Chem. High T. Scr.*, 2003, **6**, 279-286.
29. Y. Feng, A. P. Jadhav, C. Rodighiero, Y. Fujinaga, T. Kirchhausen and W. I. Lencer, *EMBO Rep.*, 2004, **5**, 596-601.
30. R. A. Spooner, P. Watson, D. C. Smith, F. Boal, M. Amessou, L. Johannes, G. J. Clarkson, J. M. Lord, D. J. Stephens and L. M. Roberts, *Biochem. J*, 2008, **414**, 471-484.
31. M. P. Nambiar and H. C. Wu, *Exp. Cell Res.*, 1995, **219**, 671-678.
32. S. Herold, H. Karch and H. Schmidt, *Int. J. Med. Microbiol.*, 2004, **294**, 115-121.
33. M. C. Erickson and M. P. Doyle, *J. Food Prot.*, 2007, **70**, 2426-2449.
34. Short SAR studies have been conducted on other membrane transport inhibitors (see ref. 20 and 26) but generally analogues derived from molecules as complex as brefeldin A are less amenable to such approaches.
35. K. Gewald, E. Schinke and H. Bottcher, *Chem. Ber.* , 1966, **99**, 94-100.
36. L. J. Guetzoyan, R. A. Spooner, J. M. Lord, L. M. Roberts and G. J. Clarkson, *Eur. J. Med. Chem.*, 2010, **45**, 275-283.
37. R. R. Rostovtsev, L. G. Green, V. V. Fokin and K. B. Sharpless, *Angew. Chem. Int. Ed.*, 2002, **41**, 2596-2599.
38. E. M. Doherty, C. Fotsch, Y. Bo, P. P. Chakrabarti, N. Chen, N. Gawa, N. Han, M. G. Kelly, J. Kincaid, L. Klionsky, Q. Liu, V. I. Ognyanov, R. Tamir, X. Wang, J. Zhu, M. H. Norman and J. J. S. Treanor, *J. Med. Chem.*, 2005, **48**, 71-90.
39. T. Pirali, S. Gatti, R. Di Brisco, S. Tacchi, R. Zaninetti, E. Brunelli, A. Massarotti, G. Sorba, P. L. Canonico, L. Moro, A. A. Genazzani, G. C. Tron and R. A. Billington, *Chem. Med. Chem.*, 2007, **2**, 437-440.
40. Q. Zhang, J. M. Takacs, S. M. Stribbling, Y. Light, J. Martin and C. J. Springer, *Org. Lett.*, 2008, **10**, 545-548.
41. G. L. Plourde and R. R. Spaetzel, *Molecules*, 2002, **7**, 697-705.
42. H. Hey and H. J. Arpe, *Angew. Chem. Int. Ed.* , 1973, **12**, 928-929.
43. K. Sandvig, I. H. Madshus and S. Olsnes, *Biochem. J*, 1984, **219**, 935-940.
44. S. Ponnambalam, M. Girotti, M. L. Yaspo, C. E. Owen, A. C. Perry, T. Suganuma, T. Nilsson, M. Fried, G. Banting and G. Warren, *J. Cell Sci.*, 1996, **109** (Pt 3), 675-685.
45. A. D. Linstedt and H. P. Hauri, *Mol. Biol. Cell*, 1993, **4**, 679-693.
46. V. D. Bock, D. Speijer, H. Hiemstra and J. H. van Maarseveen, *Org. Biomol. Chem.*, 2007, **5**, 971-975.
47. F. A. Barr, M. Puype, J. Vandekerckhove and G. Warren, *Cell*, 1997, **91**, 253-262.
48. D. T. Shima, K. Haldar, R. Pepperkok, R. Watson and G. Warren, *J. Cell Biol.*, 1997, **137**, 1211-1228.
49. L. Renault, B. Guibert and J. Cherfils, *Nature*, 2003, **426**, 525-530.
50. G. Tai, L. Lu, L. Johannes and W. Hong, *Methods Enzymol.*, 2005, **404**, 442-453.
51. L. Lu, G. Tai and W. Hong, *Mol. Biol. Cell*, 2004, **15**, 4426-4443.
52. H. W. Shin, H. Kobayashi, M. Kitamura, S. Waguri, T. Suganuma, Y. Uchiyama and K. Nakayama, *J. Cell Sci.*, 2005, **118**, 4039-4048.
53. A. Yoshino, S. R. Setty, C. Poynton, E. L. Whiteman, A. Saint-Pol, C. G. Burd, L. Johannes, E. L. Holzbaur, M. Koval, J. M. McCaffery and M. S. Marks, *J. Cell Sci.*, 2005, **118**, 2279-2293.
54. Z. Z. Lieu, M. C. Derby, R. D. Teasdale, C. Hart, P. Gunn and P. A. Gleeson, *Mol. Biol. Cell*, 2007, **18**, 4979-4991.
55. S. N. Zolov and V. V. Lupashin, *J. Cell Biol.*, 2005, **168**, 747-759.
56. F. J. Perez-Victoria, G. A. Mardones and J. S. Bonifacino, *Mol. Biol. Cell*, 2008, **19**, 2350-2362.
57. M. C. Derby, Z. Z. Lieu, D. Brown, J. L. Stow, B. Goud and P. A. Gleeson, *Traffic*, 2007, **8**, 758-773.
58. A. Girod, B. Storrie, J. C. Simpson, L. Johannes, B. Goud, L. M. Roberts, J. M. Lord, T. Nilsson and R. Pepperkok, *Nat. Cell Biol.*, 1999, **1**, 423-430.
59. J. White, L. Johannes, F. Mallard, A. Girod, S. Grill, S. Reinsch, P. Keller, B. Tzschaschel, A. Echard, B. Goud and E. H. Stelzer, *J. Cell Biol.*, 1999, **147**, 743-760.
60. S. Monier, F. Jollivet, I. Janoueix-Lerosey, L. Johannes and B. Goud, *Traffic*, 2002, **3**, 289-297.
61. M. Wilcke, L. Johannes, T. Galli, V. Mayau, B. Goud and J. Salamero, *J. Cell Biol.*, 2000, **151**, 1207-1220.
62. J. McKenzie, L. Johannes, T. Taguchi and D. Sheff, *FEBS J.*, 2009, **276**, 1581-1595.